

Europium Nanoparticles and Time-resolved Fluorescence for Ultrasensitive Detection of Prostate-specific Antigen

HARRI HÄRMÄ,* TERO SOUKKA, and TIMO LÖVGREN

Background: Nanoparticle-based detection technologies have the potential to improve detection sensitivity in miniature as well as in conventional biochemical assays. We introduce a detection technology that relies on the use of europium(III) nanoparticles and time-resolved fluorometry to improve the detection limit of biochemical assays and to visualize individual molecules in a microtiter plate format.

Methods: Streptavidin was covalently coated on 107-nm nanoparticles containing >30 000 europium molecules entrapped with β -diketones. In a model assay system, these nanoparticles were used to trace biotinylated prostate-specific antigen (PSA) in a microtiter plate format.

Results: The detection limit (mean + 3 SD of the zero calibrator) of biotinylated PSA was 0.38 ng/L, corresponding to 10 fmol/L or 60 zeptomoles (60×10^{-21} moles) of PSA. Moreover, single nanoparticles, representing individual PSA molecules, were visualized in the same microtiter wells with a time-resolved fluorescence microscope using a $\times 10$ objective. Single nanoparticles, possessing high specific activity, were also detected in solution by a standard time-resolved plate fluorometer.

Conclusions: The universal streptavidin-coated europium(III) nanoparticle label is suitable for detection of any biotinylated molecule either in solution or on a solid phase. The europium(III) nanoparticle labeling technology is applicable to many areas of modern biochemical analysis, such as immunochemical and multi-analyte DNA-chip assays as well as histo- and cytochemistry to improve detection sensitivities.

© 2001 American Association for Clinical Chemistry

Fluorescence, chemiluminescence, and bioluminescence are widely used to detect binding events in many biomedical and diagnostic analyses. The measured optical signal is typically based on an accumulated sum of labels present in a probe region. Therefore, no precise information on single molecules or on distribution and time trajectories of single molecules can be obtained. To detect single-molecule binding events, highly fluorescent labels such as single fluorescent molecules (1, 2), fluorescent nanoparticles (3), up-converting phosphors (4), quantum dots (5), and plasmon-resonant particles (6) have been studied. The low light yield of single fluorescent molecules, up-converting phosphors, and quantum dots limits the use of these techniques. Rapidly decaying fluorescence gives rise to autofluorescence and nonspecific fluorescence, further decreasing the sensitivity, and often time-dependent blinking and irreversible photodestruction restrict the use of rapidly decaying fluorescent labels. Plasmon-resonant particles possess a high light yield, but broad emission bands limit the use of these reporters, especially in simultaneous analysis of multiple target molecules. Hence, improved label technologies are still needed.

Ultra-high-throughput screening, chip-based technologies, multitarget detection systems, and diagnostic screening are rapidly growing areas, and an ongoing trend is to miniaturize these assay formats. In microarray and microspot techniques, spatial resolution of individual reactive sites on a chip becomes extremely important. At the same time, improved labeling and detection technologies are required to analyze smaller sample volumes and to measure sample on a limited solid-phase area. The use of intense fluorescence labels with high specific activity and low nonspecific signal is a prerequisite before optimal miniaturization can be accomplished. Obviously, bioimaging also benefits from such a labeling technology.

Time-resolved fluoroimmunoassays were introduced in the early 1980s (7). The high specific activity and very low background signals provided by the temporal separation of the long-lived emission signals have enabled

Department of Biotechnology, University of Turku, Tykistökatu 6, FIN-20520 Turku, Finland.

*Author for correspondence. Fax 358-2-3338050; e-mail harri.harma@utu.fi.

Received October 17, 2000; accepted December 7, 2000.

detection of analytes with superior sensitivity (7, 8). The most successful time-resolved fluorescence technology, the commercial DELFIA concept (Perkin-Elmer Life Sciences), is based on the enhanced signal produced by lanthanide ions as they are dissociated and successively entrapped by β -diketones, detergents, and synergistic agents (9). We previously have shown that 10 000 intrinsically fluorescent europium chelates (nondissociative) can be monitored on a single microparticle by a confocal time-resolved fluorometer (10). To further improve the sensitivity provided by nondissociative labels, we describe here a europium-label detection technology applicable to various bioanalyses. These nanosized polymer labels contain >30 000 europium molecules entrapped by β -diketones, which possess one of the highest quantum yields of the known lanthanide chelators. The polymer shell efficiently removes fluorescence-quenching water from the vicinity of the chelate by producing a hydrophobic environment. Furthermore, carboxylic groups on the surface of the label enable simple and convenient conjugation of virtually any biomolecule. With this technology, we demonstrate detection limits of zeptomoles for biotinylated prostate-specific antigen (PSA)¹ in a conventional microtiter format and visualization of PSA molecules in the same microtiter wells by a time-resolved microscope.

Materials and Methods

NANOPARTICLES

Europium chelate (β -diketone)-incorporated polystyrene nanoparticles, 107, 210, and 408 nm in diameter (1% solids), were obtained from Seradyn, Inc. The nanoparticles contained carboxyl groups on the surface for covalent bioconjugation.

The number of europium(III) ions in a single nanoparticle was determined by adding the nanoparticles to a 1 mL/L Triton X-100 solution or to the enhancement solution (DELFLIA; Perkin-Elmer Life Sciences). The signals obtained by the Victor 1420 multilabel counter were compared with a europium calibrator in the enhancement solution.

The time-resolved fluorescence excitation and emission spectra of nanoparticles (3 pmol/L) in 1 mL/L Triton X-100 and the spectra of europium ions (1 nmol/L) in the enhancement solution were measured with the LS5 spectrofluorometer (Perkin-Elmer Instruments).

COATING OF NANOPARTICLES WITH STREPTAVIDIN

Nanoparticles were prewashed with 10 mmol/L phosphate buffer, pH 7.0, on a Nanosep microporous centrifugal filter (300 kDa cutoff; Pall Filtron). Phosphate buffer was added to the particles, and the solution was sonicated with a tip sonicator (Labsonic U; B. Braun) at 80 W for 5 s. Carboxyl groups on the surface of nanoparticles were

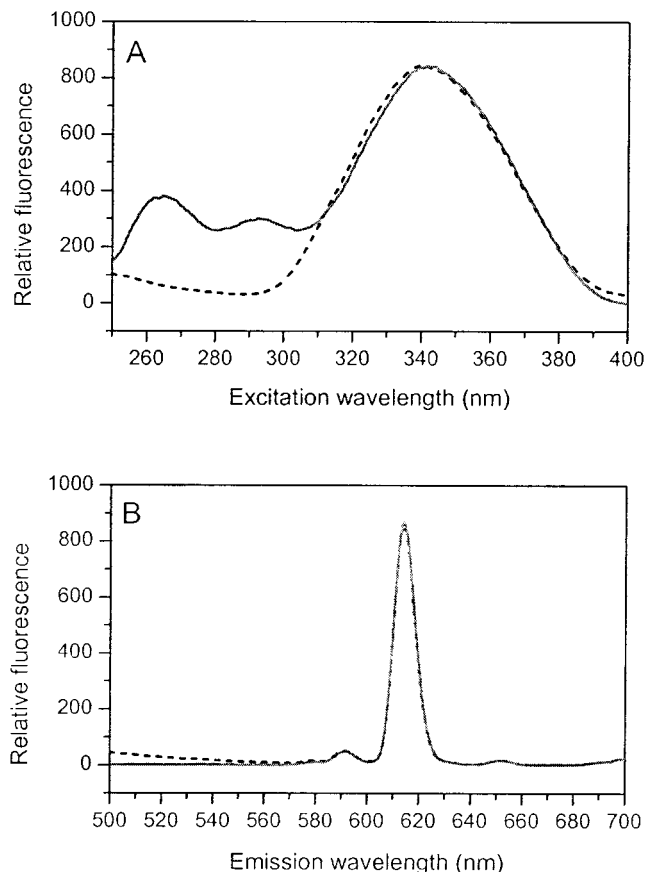


Fig. 1. Time-resolved fluorescence excitation (A) and emission (B) spectra of nanoparticles (solid line) in the 1 mL/L Triton X-100 solution or europium ions (dash line) in the enhancement solution.

activated with 10 mmol/L *N*-(3-dimethylaminopropyl)-*N'*-ethylcarbodiimide and *N*-hydroxysulfosuccinimide (Fluka) for 30 min. The activated particles were washed once with 10 mmol/L carbonate buffer, pH 9.0, and 15 μ mol/L streptavidin was added. After 2 h of incubation, the streptavidin-coated particles were washed five times with a 2 mmol/L Tris-HCl solution, pH 7.0, and stored at 4 °C.

DETECTION LIMIT OF NANOPARTICLES IN SOLUTION

The detection limits of the different-sized particles were determined with a Victor 1420 multilabel counter (Perkin-Elmer Life Sciences). Nanoparticles were diluted into the 1 mL/L Triton X-100 solution or the enhancement solution, and a 200- μ L aliquot of the nanoparticle solution was monitored. The lower limit of detection was calculated from the signal of the dilutions containing no particles (plus 3 SD).

PSA IMMUNOASSAY

PSA (100 μ g; provided by Dr. H. Lilja, Lund University Hospital, Malmö, Sweden) was biotinylated with 60 μ mol/L biotin isothiocyanate (Perkin-Elmer Life Sciences)

¹ Nonstandard abbreviations: PSA, prostate-specific antigen; mAb, monoclonal antibody; and SEM, scanning electron microscope.

in 500 μL of 50 mmol/L carbonate buffer, pH 9.8, for 2.5 h. The biotinylated PSA was separated from unbound biotin on NAP-5 and NAP-10 columns (eluted with Tris buffer). The PSA assay was carried out on an anti-PSA microtiter plate [monoclonal antibody (mAb)-H117; Perkin-Elmer Life Sciences]. In the two-step assay, 5 μL of biotinylated PSA was first incubated in 30 μL of a commercial assay buffer (Perkin-Elmer Life Sciences) for 40 min. After a washing step, 2×10^8 streptavidin-coated nanoparticles were added to the well in 40 μL (4-h incubation at room temperature). After the final wash, the quantity of the analyte was detected directly on the surface of the microtiter well with the Victor 1420 fluorometer in time-resolved mode. The detection limit of the assay was calculated based on the signal for the zero calibrator plus 3 SD.

IMAGING OF NANOPARTICLES

After the PSA dilution curves were established, the same microtiter wells (no additional sample preparation) were studied with a time-resolved fluorescence microscope to visualize PSA molecules. A Nikon Eclipse E600 light microscope (Nikon) equipped for time-resolved fluorescence imaging (flashlamp, chopper, CCD camera) was used. A rotating chopper was used to close the light path to the camera during the excitation pulse (10 μs ; wavelength, 340 nm; Xenon flashlamp; Perkin-Elmer Life Sciences) and the delay time (between excitation and light collection). Thereafter, the rotating chopper opened the light path to the camera for 600 μs (emission, 615 nm) and then closed the light path. The measurement cycle was repeated at 50 Hz for 30–45 s. A cooled scientific CCD camera (UltraPix; Perkin-Elmer Optoelectronics) was used to detect nanoparticles. The objectives used were

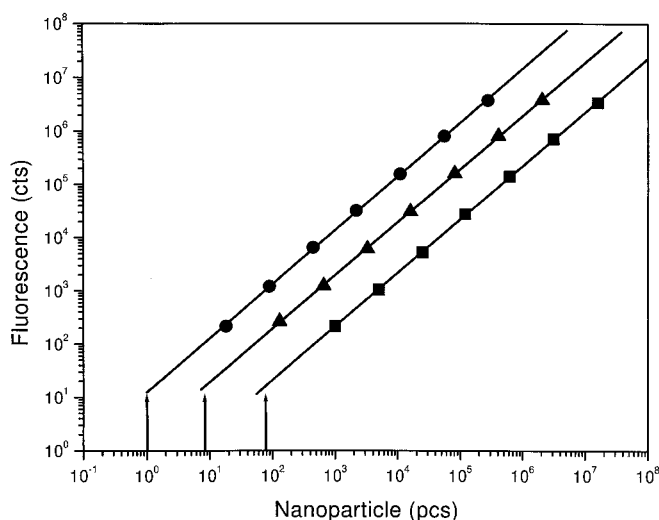


Fig. 2. Dilution curves of 107-nm (■), 210-nm (▲), and 408-nm (●) particles in the 1 mL/L Triton X-100 solution (200 μL) measured with a standard time-resolved plate fluorometer.

The arrows indicate the lower limits of detection. cts, counts.

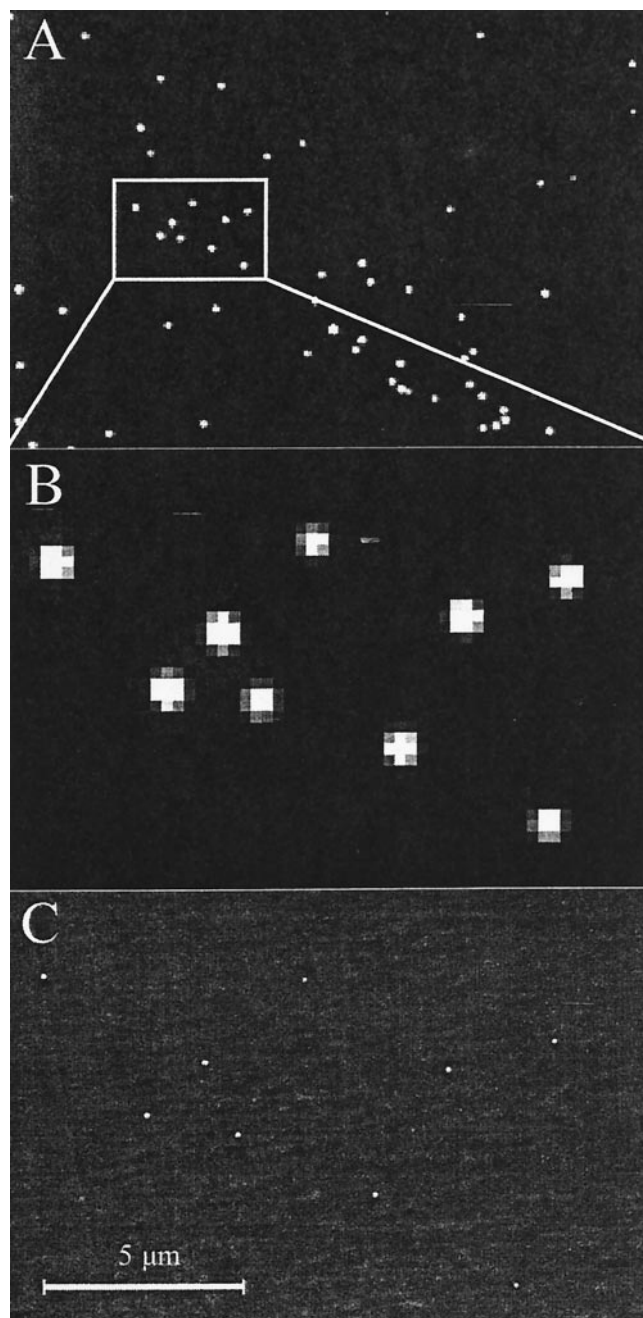


Fig. 3. Single 107-nm nanoparticle detection of the same area using time-resolved fluorescence (A and B) and SEM (C).

The magnification in the time-resolved fluorescence microscope was $\times 60$, and the exposure time was 30 s.

$\times 10$ and $\times 60$ with numerical apertures of 0.3 and 0.85, respectively. The time-resolved images were analyzed with the Image-Pro Plus, Ver. 4.0, image analysis software (Media Cybernetics).

Scanning electron microscope (SEM) images were taken with a S360 electron microscope (LEO Electron Microscopy). For the SEM images, the particles were dried on an etched-track polycarbonate filter (50 nm; Isopore; Whatman) and coated with gold.

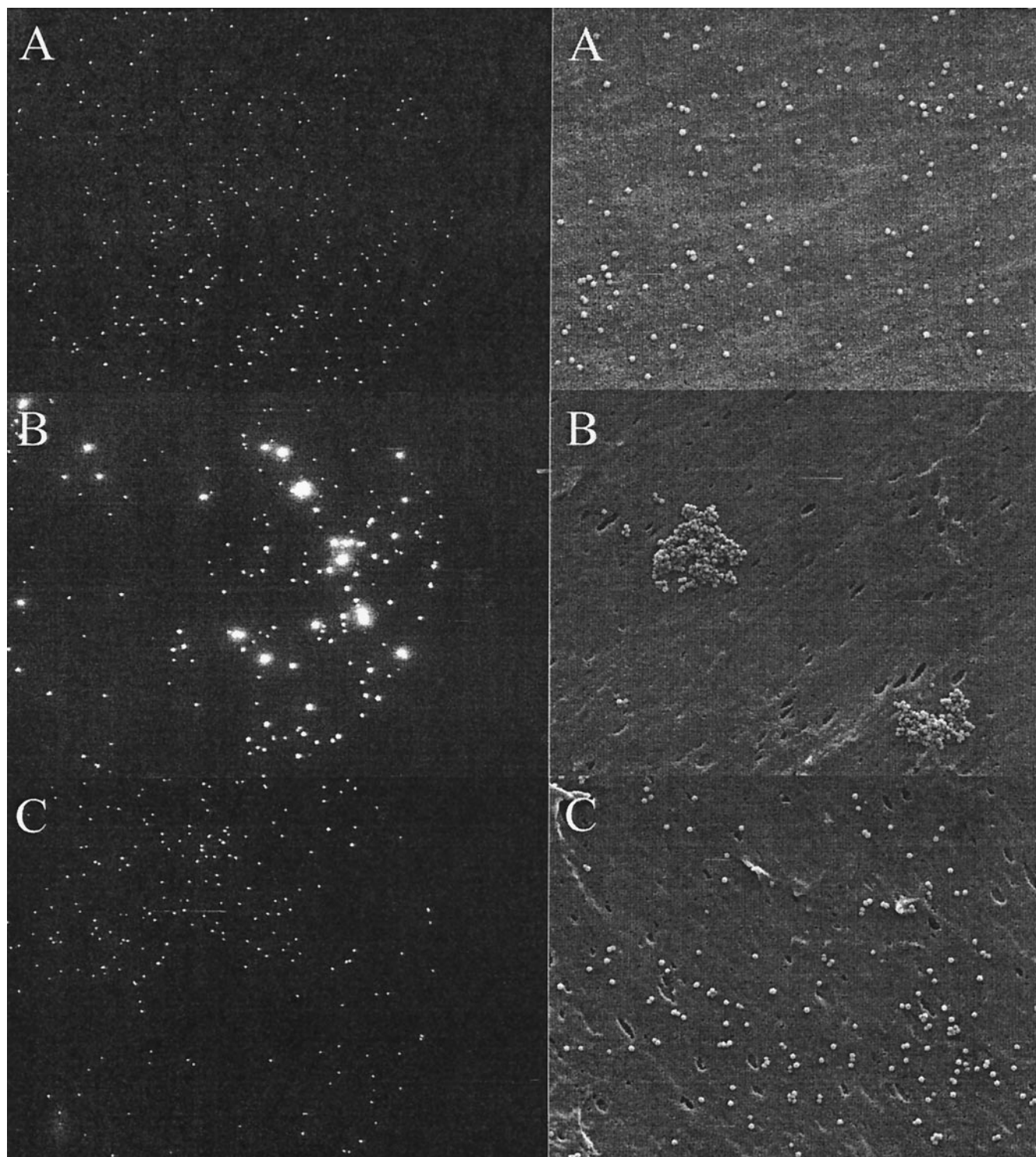


Fig. 4. Visualization of aggregation in nanoparticle suspensions using time-resolved fluorescence (*left*) and SEM (*right*).

The stock solution was nearly free of aggregates (A). Streptavidin-coated nanoparticles aggregated in 5 mol/L NaCl solution (B). Streptavidin-coated nanoparticles were essentially nonaggregated in a 2 mmol/L Tris buffer, pH 7.0 (C).

Results and Discussion

NANOPARTICLES

The number of chelated europium(III) ions in a single nanoparticle was determined by comparing the signal of a

known number of particles in the 1 mL/L Triton X-100 solution or in the enhancement solution to an europium(III) calibrator (in the enhancement solution). We found 3.1×10^4 chelated europium(III) ions in a single

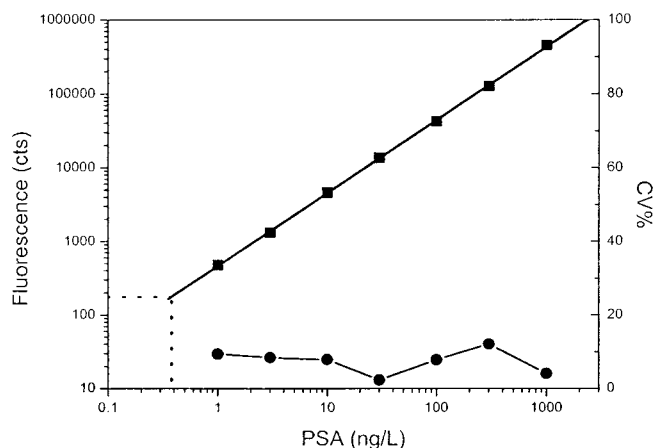


Fig. 5. Dilution curve (■) and precision profile (●) of biotinylated PSA measured with the standard time-resolved plate fluorometer.

The dashed line indicates the lower limit of detection, 0.38 ng/L, corresponding to 10 fmol/L or 60 zeptomoles of PSA. cts, counts.

107-nm nanoparticle, which was independent of the solution used: the chelating enhancement solution or the nonenhancing Triton X-100 solution. Therefore, the signal originated solely from the nanoparticles and not from free europium(III) ions in the solutions. The number of chelated europium(III) ions in the larger nanoparticles, 210 and 408 nm in diameter, were 2.5×10^5 and 2×10^6 , respectively. Fig. 1 shows that no significant difference was observed in the excitation and emission spectra of europium(III) ions in the enhancement solution or the nanoparticles in the Triton X-100 solution because the chelating ligand was the same in both solutions. The difference in the far-ultraviolet region of the excitation spectra can be attributed to the absorbance of the polystyrene polymer matrix of the nanoparticles. In addition to the measured spectra, decay times were determined for the 107-nm nanoparticle suspension in the 1 mL/L Triton X-100 solution as well as for europium(III) in the enhancement solution. Decay times of $\sim 720 \mu\text{s}$ were measured for both solutions, indicating identical coordination site occupancy of europium(III) ions in the two systems.

The signals of lanthanide chelates are known to be low, as low as 1000-fold lower than signals of rapidly decaying fluorophores, mainly because the emission light is temporally resolved and only a fraction of the emitted light is collected. The concentration of chelated europium(III) ions in the nanoparticles was $\sim 80 \text{ mmol/L}$, which would apparently cause an inner-filter effect when applied to rapidly decaying fluorophores (11). It is not uncommon that rapidly decaying fluorophores self-quench in micromolar concentrations. However, when lanthanide chelates are used, no such effect has been found even in high (millimolar) concentrations. Therefore, the loss in signal attributable to the temporally resolved emission can be effectively compensated by use of nanoparticles containing a high concentration of lanthanide chelates.

The detection limits of the nanoparticles were mea-

sured in 200 μL of the 1 mL/L Triton X-100 solution with the standard time-resolved plate fluorometer. As shown in Fig. 2, one single 408-nm nanoparticle was detected in solution, and the detection limits for the 210- and 107-nm particles were 8 and 75, respectively.

IMAGING OF NANOPARTICLES

In Fig. 3A is shown an image of nanoparticles (noncoated, 107 nm) dried on an etched-tracked membrane when a Nikon Eclipse E600 light microscope equipped for time-resolved fluorescence measurements was used for the imaging ($\times 60$ objective and 30-s exposure time). To ensure that each measured individual dot was a single particle, we dried ~ 1000 nanoparticles (calculated from particle concentration, 1% solids; diameter, 107 nm) in a small area on the membrane and took images using a $\times 10$ objective and a 45-s exposure time. Image analysis software was used to calculate the number of individual measured dots. The number of dots corresponded accurately to the assumed particle number, 1018 ± 104 (eight individual dried areas). However, the image analysis could not solely ensure that each dot was a single particle molecule. Therefore, we compared images of nanoparticles in the time-resolved fluorescence microscope (Fig. 3, A and B) and in the SEM (Fig. 3C). These images clearly demonstrated that each measured dot in the microscope image was, indeed, a single nanoparticle.

Nanosized particles are commonly used in agglutination tests. In these tests, it is desired that the particles aggregate when exposed to analyte. In many assay concepts, aggregation is not, however, a desired property. Although nanosized labels have been used in several single-molecule imaging, DNA, and immunoassay studies, very little information, if any, has been given about the obvious aggregation problem. Because the time-resolved fluorescence microscope allowed quantitative particle counting, we had strict control over the nanoparticle suspensions used, as exemplified in Fig. 4: noncoated (Fig. 4A), aggregated streptavidin-coated (Fig. 4B), and nonaggregated streptavidin-coated (Fig. 4C) nanoparticles measured with a time-resolved fluorescence microscope and SEM. If the assays were performed with an aggregated particle suspension, it would be obvious that the number of single nanoparticles was not accurate, and no reliable results could be obtained. To demonstrate this effect, the noncoated nanoparticles were diluted first with H_2O or 5 mol/L NaCl solution and subsequently 10 000-fold with the 1 mL/L Triton X-100 solution. Because a high sodium concentration is known to aggregate nanosized carboxyl particles, the final dilution of the NaCl-treated solution was assumed to be highly aggregated. The non-NaCl-treated and NaCl-treated solutions measured in the standard time-resolved plate fluorometer yielded the same signals (data not shown). However, the CVs varied significantly. For the non-NaCl-treated and NaCl-treated nanoparticle solutions, the CVs were 0.4%

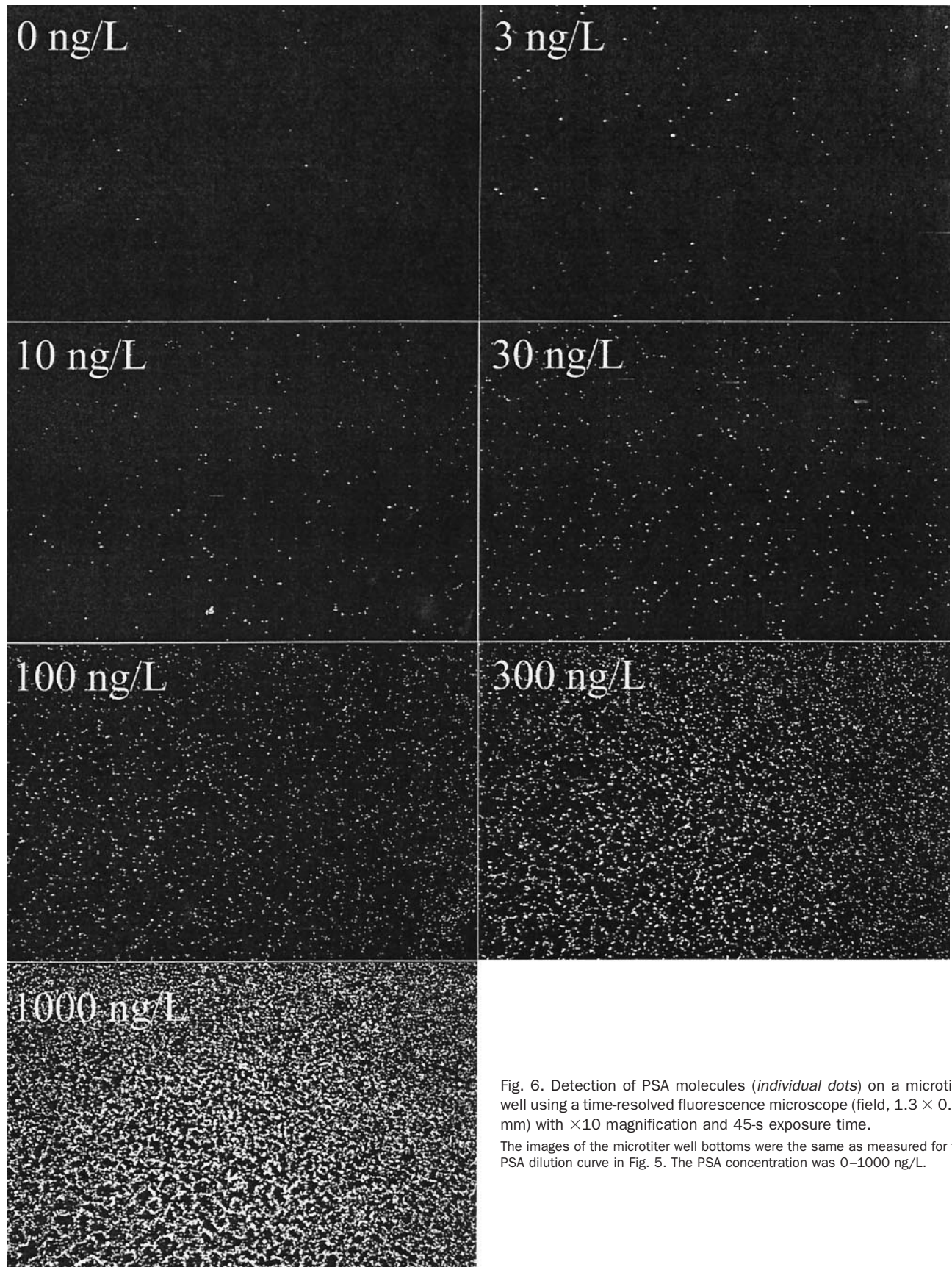


Fig. 6. Detection of PSA molecules (*individual dots*) on a microtiter well using a time-resolved fluorescence microscope (field, 1.3×0.97 mm) with $\times 10$ magnification and 45-s exposure time.

The images of the microtiter well bottoms were the same as measured for the PSA dilution curve in Fig. 5. The PSA concentration was 0–1000 ng/L.

and 21%, respectively, when six individual measurements were compared.

PSA IMMUNOASSAY

A model PSA assay was performed on a microtiter plate coated with a PSA-specific mAb [mAb-H117 (12)]. Biotinylated PSA was incubated in the first assay step, followed by a second incubation with streptavidin-coated 107-nm nanoparticles. The analyte reaction volume was small (30 μ L) because we wanted PSA to react on the bottom of the plate for direct surface detection. In this concept, no additional enhancement step was required. Fig. 5 shows the dilution curve of the PSA assay. The response was linear over three orders of magnitude. The lower limit of detection was 0.38 ng/L, corresponding to 10 fmol/L or 60 zeptomoles (60×10^{-21} moles) of PSA molecules. This is more than 10-fold lower than the previously reported molecule quantity in a microtiter plate-based PSA assay (0.38 ng/L for a 5- μ L sample vs 1 ng/L for a 50- μ L sample) (13). The present PSA assay setup cannot be considered a true assay because the analyte was biotinylated.

To perform a true noncompetitive sandwich PSA assay, we biotinylated a second PSA-specific mAb (mAb-5A10). This work (14) was a continuation of the work presented here. The detection limit was 1.6 ng/L, which is not significantly lower than that of the present assay, although this assay concept suffered from increased nonspecific binding produced by the additional tracer molecule, biotinylated mAb-5A10. The incubation time of streptavidin-coated nanoparticles with the surface-bound biotinylated mAb corresponding to the analyte concentration was short, 5 min. We have also theoretically and experimentally studied the kinetics of the nanoparticles in a sandwich-type assay format and found that confining the number of surface-coupled antibodies or other biospecific binding reactants, such as streptavidin, to the nanoparticles produced enhanced association rate constants when compared with a soluble biospecific binding reactant (Soukka T, Härmä H, Paukkunen J, Lövgren T. Immunoassays based on multivalent nanoparticle-antibody bioconjugates utilize kinetically enhanced monovalent binding affinity. Submitted for publication).

In Fig. 6, images of the same microtiter wells measured for the biotinylated PSA dilution curve (above) were taken with the time-resolved fluorescent microscope using a $\times 10$ objective and a 45-s exposure time. The calculated number of individual nanoparticles (Image-Pro analysis software) followed the concentration of PSA as anticipated, producing a dilution curve with a lower limit of detection, 0.8 ng/L, that was in a good agreement with the result measured with the standard time-resolved plate fluorometer. With this technology, imaging of individual PSA molecules was possible, although the practical limit of the assay was defined by nonspecific binding and single molecules were detected only in principle.

At the lower limit of detection, 35 000 PSA molecules

were detected, and hence, in the probe area of the microscope ($\times 10$ objective; 1.3 mm²), 650 nanoparticles representing PSA molecules should have been found (estimated area for 30- μ L volume was 70 mm²). However, the number of nanoparticles found in the microscope image was <5% of the estimated amount at the lower limit of detection. Obviously, the large size of the nanoparticles restricted somewhat the access of nanoparticles to every PSA molecule on the surface, and the random coupling of biotin through the primary amines of PSA was also likely to cause steric hindrance. Furthermore, very small amounts of streptavidin or streptavidin fragments were apparently present in solution. It is not difficult to imagine that some tetrameric streptavidin molecules or streptavidin fragments dissociated from the nanoparticle surface when the total number of streptavidin in one assay was in the order of 10^{11} . The soluble streptavidin molecules bound fast and without restricted accessibility to biotinylated analyte. In conventional assays, the dissociation of streptavidin would not be detectable because the sensitivities of these assays would not allow distinguishing of very small quantities of analyte. If these factors influencing the reduced efficiency of the PSA detection can be controlled, a more than 10-fold improvement in the lower limit of detection could possibly be reached.

PSA molecules with nanosized time-resolved fluorescent labels in a microtiter plate format were imaged with a $\times 10$ objective. With this objective, no specialized reaction well was required for the detection of PSA because the working distance of the objective was large, 16 mm. We used a 45-s exposure time to image the nanoparticles, but the individual nanoparticles were visible after a 1-s exposure. The longer exposure time was used only for demonstration purposes to improve the signal-to-noise ratio (>100 with a $\times 10$ objective and 45-s exposure time). Because a shorter exposure time can be applied, a more than 2-fold (10-fold reduced europium content on one nanoparticle) smaller particle size could be used to detect analyte molecules, which in turn makes the nanoparticle approach more suitable for other imaging technologies, such as cyto- and histochemistry.

In conclusion, we have introduced a detection technology based on nanosized europium(III) particles. Biotinylated PSA was detected with a detection limit of 60 zeptomoles in a microtiter plate format using a standard time-resolved plate fluorometer, and individual PSA molecules were visualized with a time-resolved microscope. Clearly, microarray and microspot technologies could benefit from the use of these intense time-resolved fluorescent labels in biochemical analyses, e.g., detecting subtle variations in the expression of mRNA, as well as imaging technologies such as cyto- and histochemistry. Multiplex measurements could also be performed with the current labeling technology because terbium(III), samarium(III), or dysprosium(III), all well known and characterized in

solution with chelating ligands, can be used instead of europium(III) on nanoparticles. As the time-resolved labeling technology has improved and become more familiar over the years, the detection technology has also gained more interest among instrument manufacturers. Consequently, a high-sensitivity time-resolved labeling technology such as the current nanoparticle approach could be readily implemented in any standard laboratory.

This work was supported by the State Technical Development Center of Finland (TEKES) and the Graduate School of Bioorganic Chemistry in Finland.

References

1. Unger M, Kartalov E, Chiu C-S, Lester HA, Quake SR. Single-molecule fluorescence observed with mercury lamp illumination. *Biotechniques* 1999;27:1008–14.
2. Weiss S. Fluorescence spectroscopy of single biomolecules. *Science* 1999;283:1676–83.
3. Taylor JR, Fang MM, Nie S. Probing specific sequences of single DNA molecules with bioconjugated fluorescent nanoparticles. *Anal Chem* 2000;72:1979–86.
4. Zijlmans HJMAA, Bonnet J, Burton J, Kardos K, Vail T, Niedbala RS, Tanke HJ. Detection of cell and tissue surface antigens using up-converting phosphors: a new reporter technology. *Anal Biochem* 1999;267:30–6.
5. Chan WCW, Nie S. Quantum dot bioconjugates for ultrasensitive nonisotopic detection. *Science* 1998;281:2016–8.
6. Schultz S, Smith DR, Mock JJ, Schultz DA. Single-target molecule detection with nonbleaching multicolor optical immunolabels. *Proc Natl Acad Sci U S A* 2000;97:996–1001.
7. Siitari H, Hemmilä I, Soini E, Lövgren T, Koistinen V. Detection of hepatitis B surface antigen using time-resolved fluoroimmunoassay. *Nature* 1983;301:258–60.
8. Ekins RP, Dakubu S. The development of high sensitivity pulsed light, time-resolved fluoroimmunoassays. *Pure Appl Chem* 1985; 57:473–82.
9. Soini E, Lövgren T. Time-resolved fluorescence of lanthanide probes and application in biotechnology. *CRC Crit Rev Anal Chem* 1987;18:105–54.
10. Lövgren T, Heinonen P, Lehtinen P, Hakala H, Heinola J, Harju R, et al. Sensitive bioaffinity assays with individual microparticles and time-resolved fluorometry. *Clin Chem* 1997;43:1937–43.
11. Lakowicz JR. Principles of fluorescence spectroscopy. New York: Plenum Press, 1983:44–7.
12. Piironen T, Villoutreix BO, Becker C, Hollingsworth K, Vihinen M, Bridon D, et al. Determination and analysis of antigenic epitopes of prostate specific antigen (PSA) and human glandular kallikrein 2 (hK2) using synthetic peptides and computer modeling. *Protein Sci* 1998;7:259–69.
13. Ferguson RA, Yu H, Kalyvas M, Zammit S, Diamandis EP. Ultra-sensitive detection of prostate-specific antigen by a time-resolved immunofluorometric assays and the Immulite immunochemiluminescent third-generation assays. *Clin Chem* 1996;42:675–84.
14. Härmä H, Soukka T, Lönnberg S, Paukkunen J, Tarkkinen J, Lövgren T. Zeptomole detection sensitivity of prostate-specific antigen in a rapid microtiter plate assay using time-resolved fluorescence. *Luminescence* 2000;15:351–5.